Supporting Information

Theoretical Investigations of the Chemical Bonding in $MM'O_2$ Clusters (M, M′ = Be, Mg, Ca)

Robert Ponec[1*] and David Cooper[2]

[1]Institute of Chemical Process Fundamentals, Czech Academy of Sciences Prague 6, Suchdol 2, 165 02 Czech Republic

[2]Department of Chemistry, University of Liverpool, Liverpool L69 7ZD, UK

*Corresponding author: PONEC@icpf.cas.cz

Contents

S1 Correlation of $r_{MM'}$ with $\theta_{MOM'}$.

As can be seen from Figure S1, we observe a very strong quadratic correlation of $r_{MM'}$ with $\theta_{MOM'}$, such that R^2 is almost unity and the root mean square deviation in the predicted angle is less than 0.08°. [Note that values of $r_{MM'}$ and $\theta_{MOM'}$ are used here with more decimal places than are quoted in Table 1.] The underlying reason for this very strong quadratic correlation is likely to be trigonometric identities that apply to such an orthodiagonal quadrilateral (namely a kite).

Figure S1. Correlation of $r_{MM'}$ with $\theta_{MOM'}$ for the $MM'O_2$ clusters. The dotted curve is a quadratic.

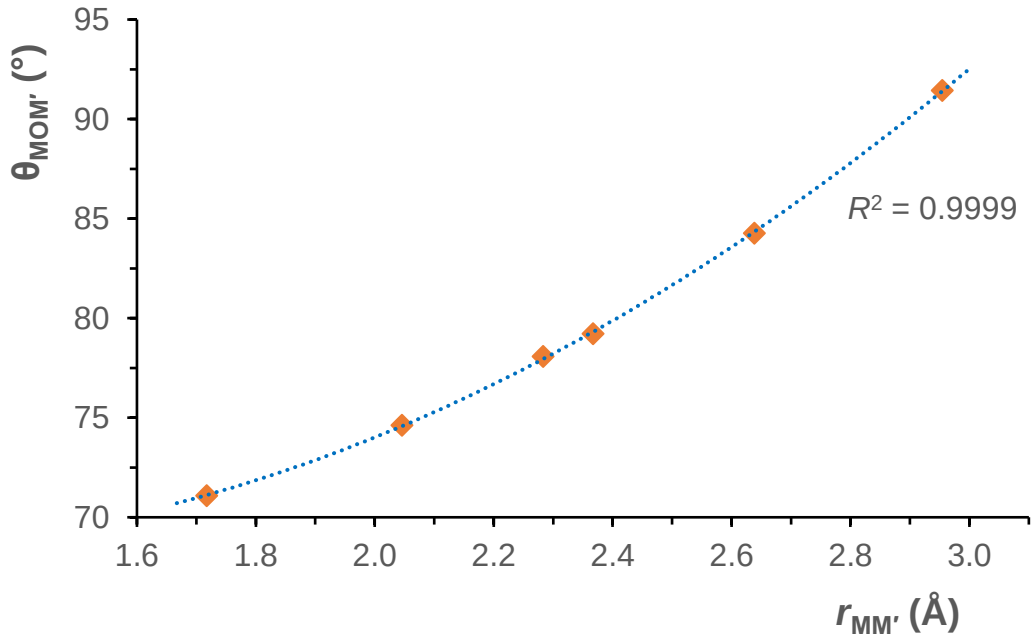

S2 Results of additional energy calculations and geometry optimizations.

Table S1. Dissociation energies to metal oxide monomers calculated at the all electron CCSD/cc-pVTZ optimized geometries using frozen core CCSD(T)/cc-pVQZ. See also Table 2.

	D_e (kcal/mol)
Be_2O_2	163
$BeMgO_2$	152
Mg_2O_2	130
$MgCaO_2$	127
Ca_2O_2	121
$BeCaO_2$	157

Table S2 Results of additional geometry optimizations for $MM'O_2$ clusters, including dissociation energies to metal oxide monomers.

(a) B3LYP/cc-pVTZ

M	M′	$r_{MM'}$ (Å)	$\theta_{MOM'}$ (°)	D_e (kcal/mol)
Be	Be	1.721	71.2	162
Be	Mg	2.064	74.9	154
Mg	Mg	2.367	79.2	135
Mg	Ca	2.652	85.1	127
Ca	Ca	2.956	92.7	113
Be	Ca	2.290	78.8	155

(b) B3LYP/SDD

M	M′	$r_{MM'}$ (Å)	$\theta_{MOM'}$ (°)	D_e (kcal/mol)
Be	Be	1.844	73.9	145
Be	Mg	2.166	77.0	148
Mg	Mg	2.499	81.9	137
Mg	Ca	2.730	87.4	132
Ca	Ca	2.993	93.9	121
Be	Ca	2.357	80.6	152

(c) Monomer optimizations using B3LYP with different basis sets

M	r_{MO} (Å)	
	cc-pVTZ	SDD
Be	1.323	1.371
Mg	1.743	1.780
Ca	1.811	1.833

S3 Traditional two-center Wiberg-Mayer indices.

Table S3. Traditional two-center Wiberg-Mayer indices ($\acute{W}_{MM'}$) for $MM'O_2$ decomposed into relative contributions from the σ and π systems. See also Table 3.

M	M′	$\acute{W}_{MM'}$		
		σ	π	total
Be	Be	73%	27%	0.286
Be	Mg	69%	31%	0.197
Mg	Mg	60%	40%	0.136
Mg	Ca	61%	39%	0.160
Ca	Ca	67%	33%	0.219
Be	Ca	57%	43%	0.164

S4 Symmetry-unique valence LNOs for $MM'O_2$ clusters.

Figure S2. Symmetry-unique valence LNOs for Be_2O_2. (Molecular orientation as in Figure 1)

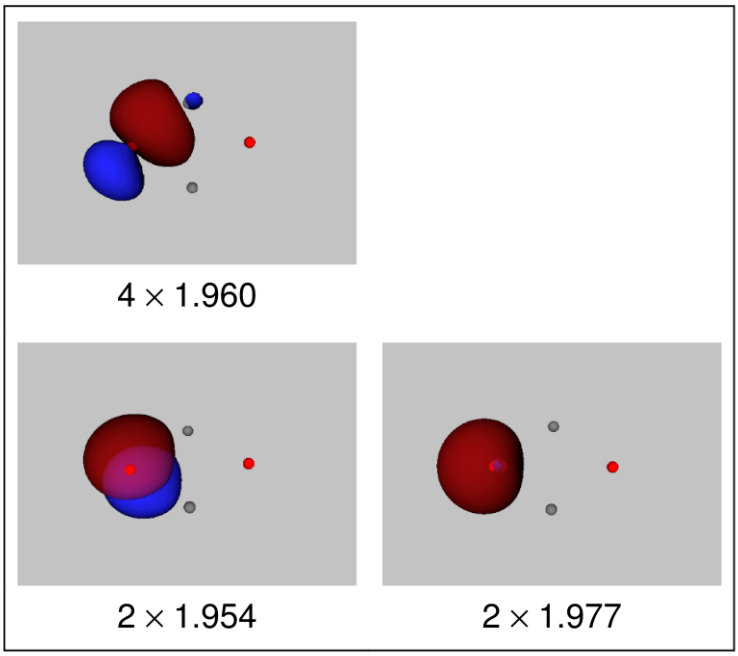

Figure S3. Symmetry-unique valence LNOs for $BeMgO_2$. (Molecular orientation as in Figure 1)

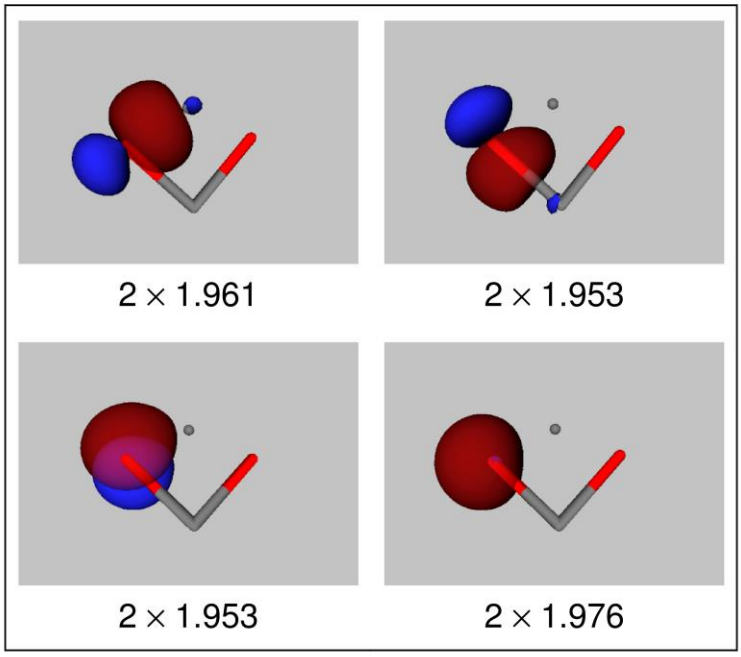

Figure S4. Symmetry-unique valence LNOs for $BeCaO_2$. (Molecular orientation as in Figure 1)

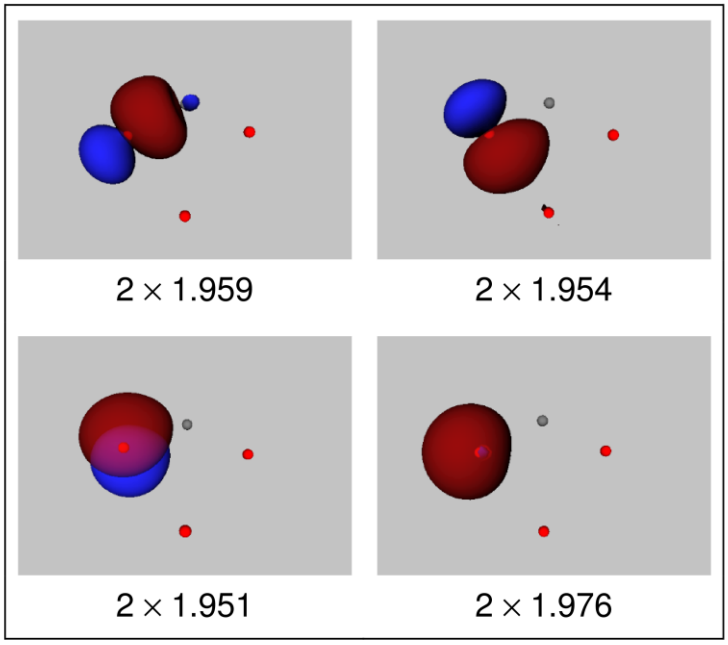

Figure S5. Symmetry-unique valence LNOs for Mg_2O_2. (Molecular orientation as in Figure 1)

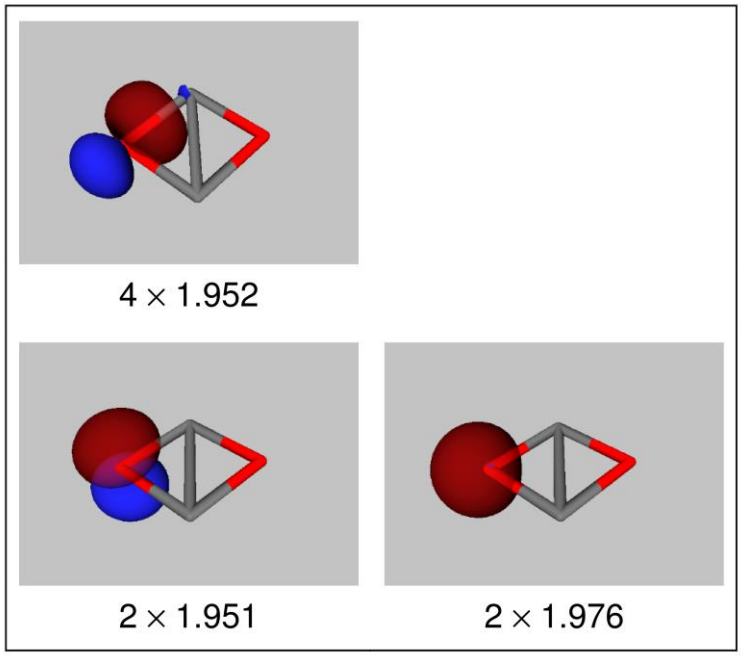

Figure S6. Symmetry-unique valence LNOs for $MgCaO_2$. (Molecular orientation as in Figure 1)

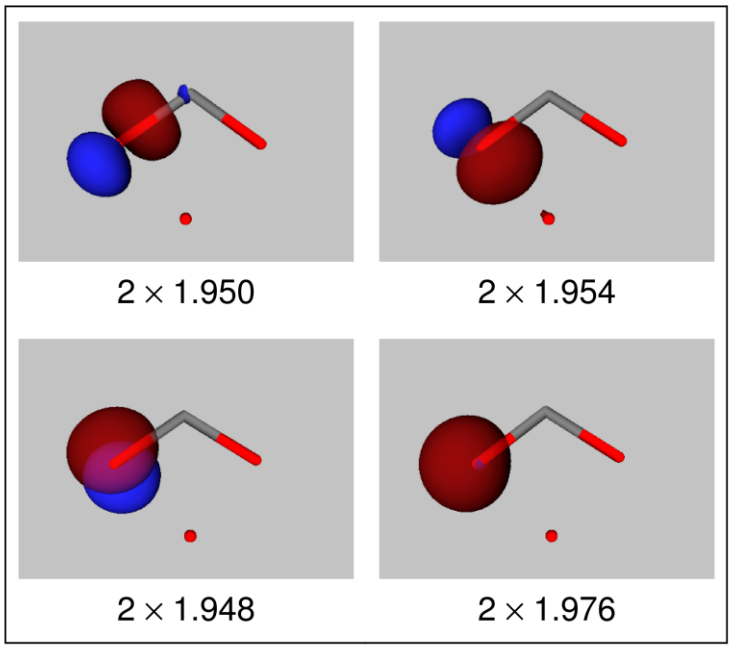

Figure S7. Symmetry-unique valence LNOs for Ca_2O_2. (Molecular orientation as in Figure 1)

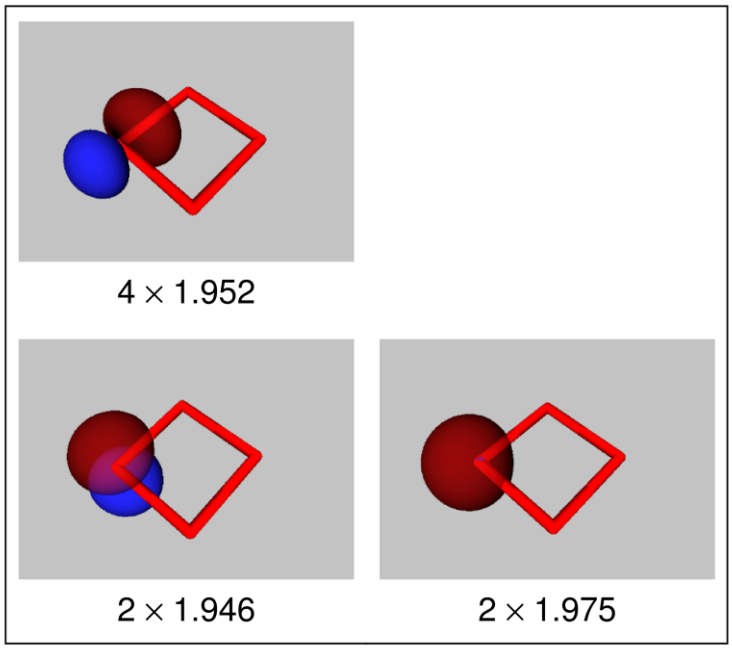

S5 Broken valences resulting from DAFH analysis for the MM′ domain and for one of the O domains in $MM'O_2$ clusters.

Figure S8. Broken valences resulting from DAFH analysis for the BeBe domain and for one of the O domains in Be_2O_2. (Molecular orientation as in Figure 1)

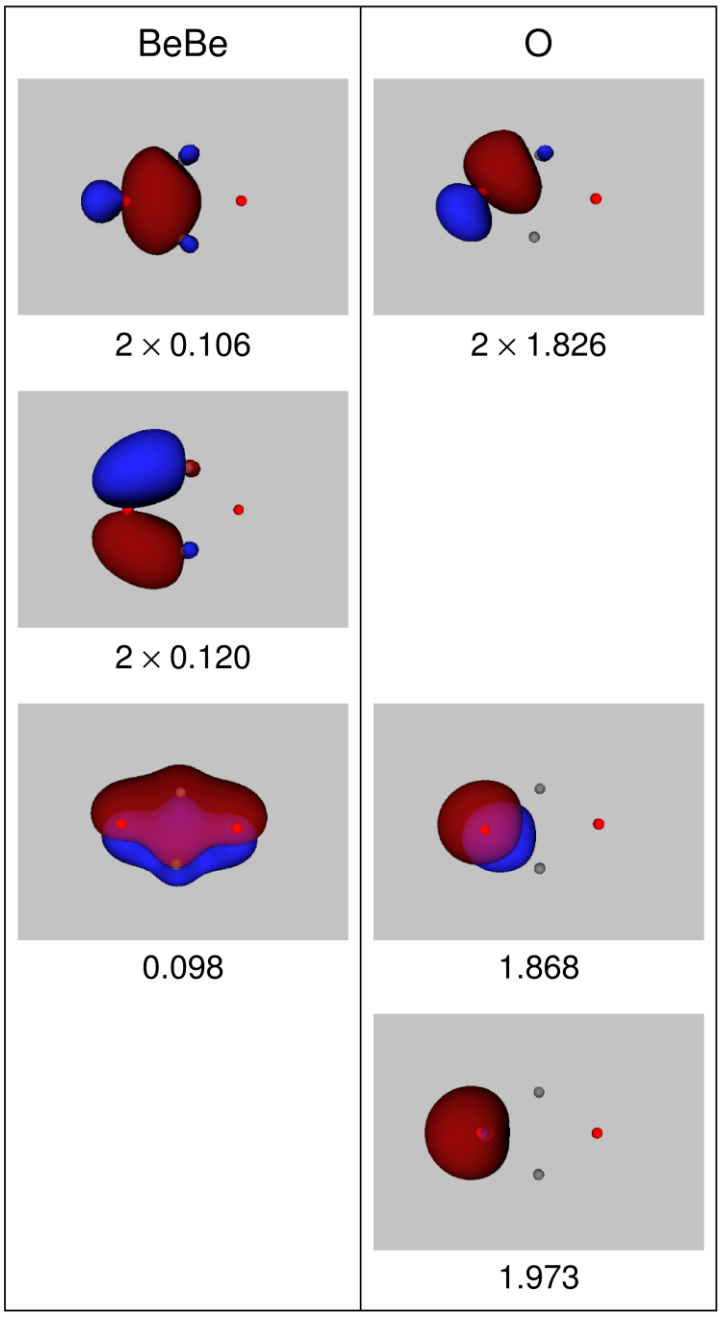

Figure S9. Broken valences resulting from DAFH analysis for the BeMg domain and for one of the O domains in $BeMgO_2$. (Molecular orientation as in Figure 1)

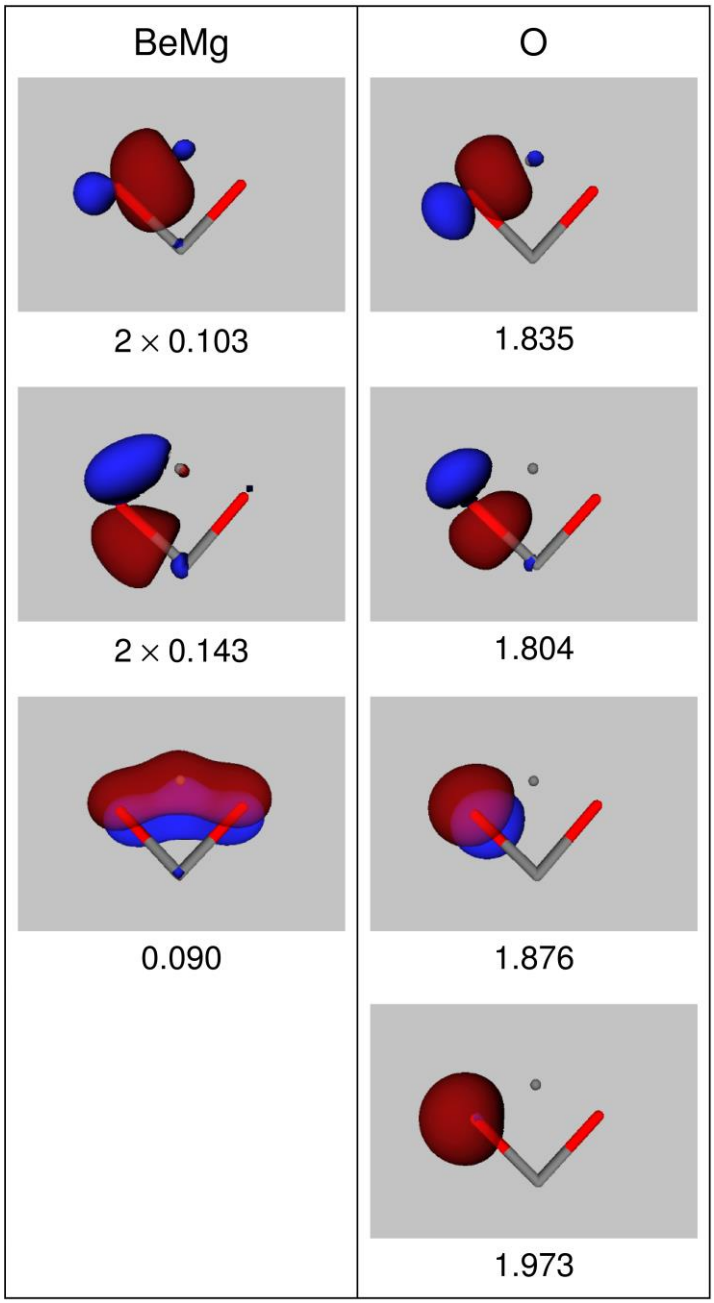

Figure S10. Broken valences resulting from DAFH analysis for the BeCa domain and for one of the O domains in $BeCaO_2$. (Molecular orientation as in Figure 1)

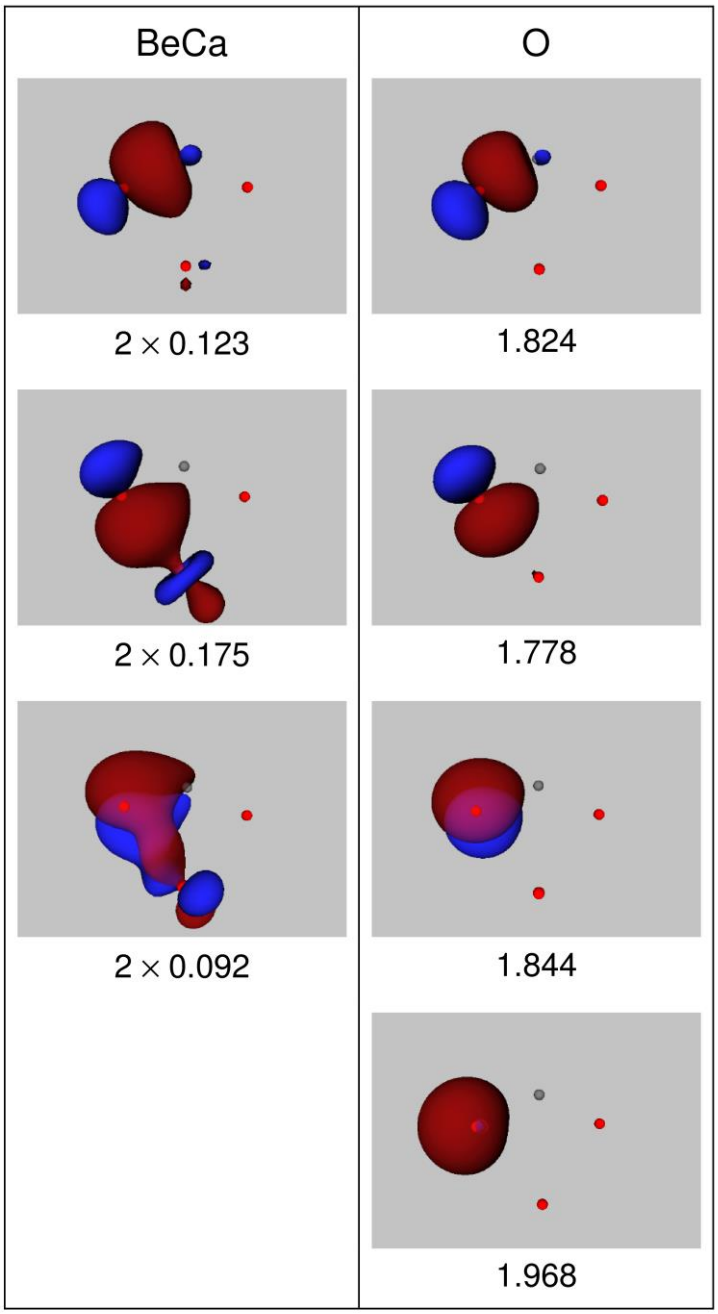

Figure S11. Broken valences resulting from DAFH analysis for the MgMg domain and for one of the O domains in Mg_2O_2. (Molecular orientation as in Figure 1)

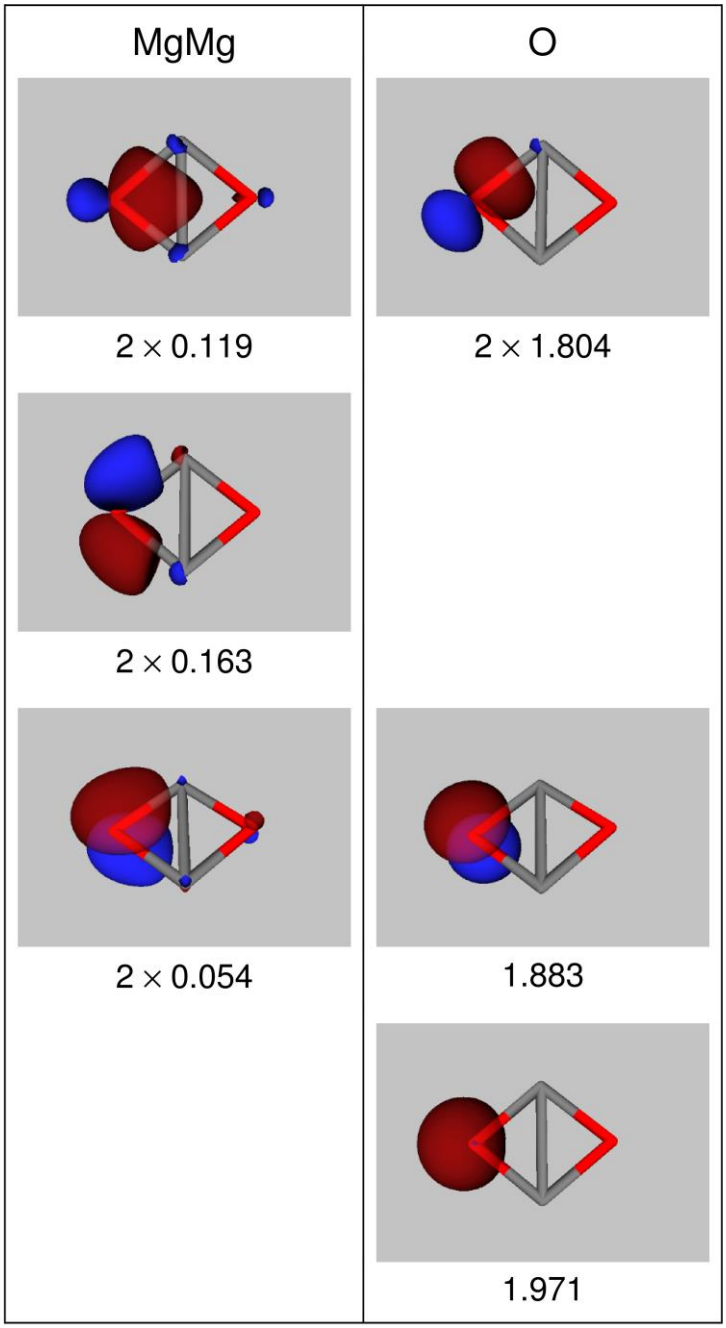

Figure S12. Broken valences resulting from DAFH analysis for the MgCa domain and for one of the O domains in $MgCaO_2$. (Molecular orientation as in Figure 1)

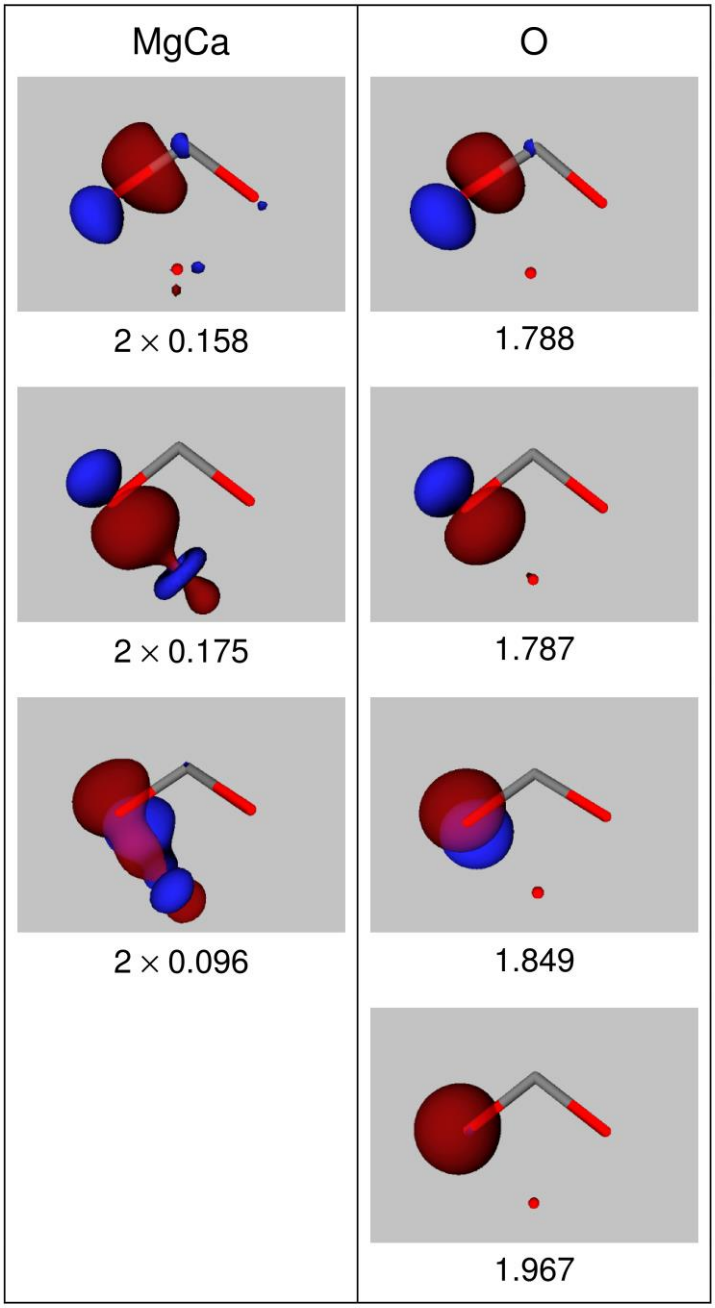

Figure S13. Broken valences resulting from DAFH analysis for the CaCa domain and for one of the O domains in Ca_2O_2. (Molecular orientation as in Figure 1)

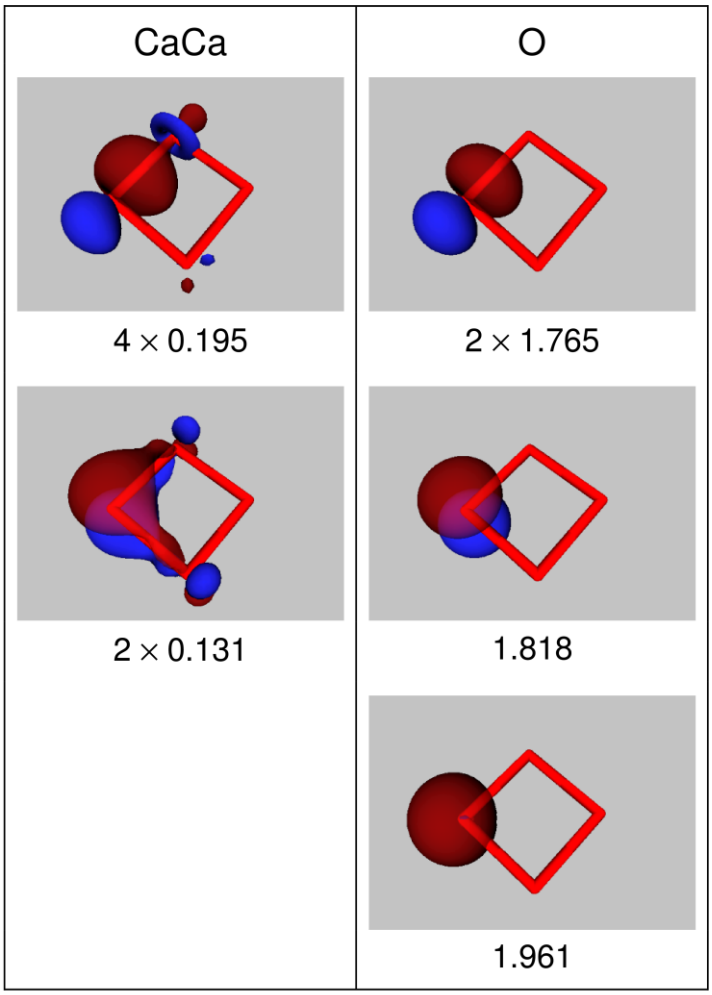

S6 Results from a heuristic 3c generalization of Cioslowski's covalent bond order.

In order to get more insight into the parentage of the weak 3c bonding, especially that in the σ system, we use a heuristic 3c generalization [23] of Cioslowski's covalent bond order [48], beyond the scope of traditional 2c-2e bonding. This straightforward generalization to three centers takes the simple form [23]:

$$\mathcal{C}(A,B,C) = 3! \sum_i {\nu_i}^3 \langle\lambda_i|\lambda_i\rangle_{\Omega_A}\langle\lambda_i|\lambda_i\rangle_{\Omega_B}\langle\lambda_i|\lambda_i\rangle_{\Omega_C} \tag{S1}$$

in which the λ_i are again the LNOs with populations ν_i that result from isopycnic localization [26] of the CCSD/cc-pVTZ natural orbitals. A particularly useful feature of such a definition is that, in contrast to the Wiberg-Mayer-like bond orders that we have used, the values of $\mathcal{C}(A,B,C)$ can be

unambiguously decomposed into contributions associated with individual LNOs. The results of such a decomposition for each of the clusters (see Table S4) clearly show that the dominant component of the weak 3c bonding in the MOM′ moieties is consistently attributed to the contributions of adjacent metal-oxygen σ bonds. There are smaller contributions in each case from the distorted $O(2p_\pi)$ LNO, with the contribution of the distorted $O(2s^2)$ quasi-lone pair being practically marginal. It follows that the indirect MM′ interactions in each MOM′ moiety arise primarily from the electron 'pairs' of adjacent metal-oxygen σ bonds with a smaller additional contribution from the $O(2p_\pi)$ electron pair that is deformed towards M and M′. This corroborates the classification of the weak 3c MOM′ interactions as predominantly 3c-4e σ bonding augmented by a smaller component due to 3c-2e π bonding.

Table S4. Relative contributions to the values of $\mathcal{C}$(M,O,M′) (see Equation S1) for $MM'O_2$ clusters from terms involving individual LNOs.

M	M′	σ(M−O)	σ(M′−O)	$O(2p_\pi)$	others
Be	Be	41%	41%	16%	2%
Be	Mg	30%	54%	15%	1%
Mg	Mg	42%	42%	14%	1%
Mg	Ca	46%	34%	19%	1%
Ca	Ca	38%	38%	24%	1%
Be	Ca	33%	45%	21%	1%